



Synthesis and Bioactivity Evaluation of Indole-Thiophene polymer with Molecular Docking Studies



Rasha A. Baseer^{a*}, Ahmed A. Abd-Rabou^{b, c}, Eman S. Zarie^d, Rasha A.M Azouz^e, Heba M. Abo-Salem^f

^a Department of Polymers and Pigments, ^b Hormones Department, ^c Stem Cell Laboratories, Center of Excellence for Advanced Science, ^d Therapeutic Chemistry Department, ^e Department of Molecular Biology, ^f Chemistry of Natural Compounds Department, National Research Centre, 12622 Dokki, Giza, Egypt.

Abstract

Emulsion polymerization of 2-amino-4-(1-benzyl-1H-indol-3-yl) thiophene-3-carbonitrile (ABITC) using ammonium persulfate (APS) afforded two isomers of (PABITC) with high molecular weight. Chemical structure and morphology of the synthesized polymers were investigated by IR, ¹HNMR, SEM, and GPC. Nano-capsulation of ABITC, PABITC, and PABITC/Doxorubicin by polyethylene glycol (PEG) was achieved by the nano-precipitation method. The anti-proliferative activity of the PABITC and nano-capsulation against HepG2, Huh7, and A549 cancer cell lines were investigated using MTT assay. The result obtained indicates that the encapsulation of ABITC inside PEG-NP led to an improvement in their anti-proliferative activity against cancer cell lines compared to ABITC. The PABITC revealed moderate anti-proliferative activity against tested cells and their encapsulation form with PEG-NP revealed no significant change in the activity. Furthermore, the anti-proliferative activity of PABITC-NP was improved after Doxorubicin (DOX) encapsulation against tested cells compared to PABITC - PEG-NP. In addition, PABITC exhibited potent antibacterial activity against tested microbes comparing to ABITC and amikacin. Moreover, the binding mode of the ABITC beside two repeated units inside the active site of the DNA gyrase B chain (PDB ID: 1KIJ) as promising bacterial target and CDK2 enzyme (PDB ID: 1PYE)] as promising cancer target was studied using molecular docking technique.

Keywords: Polymerization; Indole; Thiophene; Nano-capsule; Anti-proliferative; Antibacterial

1. Introduction

Cancer is a generic term for a massive group of diseases that can attack any part of the human body and the second leading cause of death in the world [1, 2]. In 2018, cancer was responsible for about 9.6 million deaths globally. Nearly 70% of deaths from cancer occur in low- and middle-income countries [1].

For a very long time, chemotherapies were used for treating different cancer types. However, these treatment approaches are becoming increasingly ineffective due to severe side effects and multidrug resistance[2]. Consequently, there is an urgent need to develop more effective and safer anticancer agents that can fight cancer aggressiveness[2]. Over the last decades, natural and synthetic polymers such as

*Corresponding author e-mail: ra.abdelbasser@nrc.sci.eg, rasha.daaader@gmail.com.

Receive Date: 19 July 2020, Revise Date: 08 August 2020, Accept Date: 10 August 2020

DOI: 10.21608/EJCHEM.2020.36373.2751

©2021 National Information and Documentation Center (NIDOC)

proteins, chitosan, alginate, polyethylene glycol (PEG) and poly (ϵ -caprolactone) (PCL) have great attention in the bio-applications due to their biocompatibility, controllable degradation rate and their degradation into non-toxic components [3, 4]. Recently, the active pharmaceutical ingredient contains both hydrophobic and hydrophilic functionalities (amphiphilic polymers) has been gained the attention of many scientists[5, 6, 7]. S. Barbosa's team [4] reported that poly (butylene oxide) block copolymers can be used for dissolving and chemically protecting the antitumoral drug doxorubicin. Meidong Lang's team[8] studied the optimization of poly (ethylene glycol)-b-poly(ϵ -caprolactone) (PEG-b-PCL)-based amphiphilic block copolymers for achieving a better micellar drug delivery system (DDS) with improved solubilization and delivery of doxorubicin (DOX). Several studies revealed that the solubility of active pharmaceutical ingredients can be increased by the preparation of nanoparticles and by optimization of physicochemical properties [9, 10, 11]. Besides, indole and thiophene derivatives have wide range of pharmacological activity including anticancer, antimicrobial and anti-inflammatory [12, 13, 14, 15, 16, 17, 18, 19].

In light of this feedback, our work aimed at synthesized new indole-thiophene polymers; PABITC, PEG/PABITC nano-capsules, and PEG/PABITC/Doxorubicin nano-particles and evaluated their anti-proliferative and anti-microbial activity. Also, the molecular docking studies of monomer ABITC and two repeated units of monomer (ABITC)₂ were conducted against the active site of the DNA gyrase B chain (PDB ID: 1KIJ) as promising bacterial target and CDK2 enzyme (PDB ID: 1PYE)] as promising cancer target to investigate their binding interactions.

2. Experimental

2.1. Chemicals and Supplies

All reagents and solvents were of analytical grade. 3-Acetyl indole, sodium carboxymethyl cellulose (SCMC), macrogol 6000 (PEG), sodium carboxymethyl cellulose (SCMC), sodium carboxymethyl dextran (SCMD) and MTT (3-[4, 5-dimethylthiazol-2-yl]-2.5-diphenylterazolium bromide) were purchased from Sigma Aldrich (St Louis, MO, USA). Ammonium persulfate (APS) and sodium dodecylbenzene sulfonate (SDBS) were

obtained from El-Nasr pharmaceutical chemicals co. (Egypt).

2.2. Spectral and Physical Characterization of new indole-thiophene polymer

IR spectra were performed on a Beckman infrared spectrophotometer PU 7712 using KBr disk (United States). The ¹H NMR spectra were measured on Bruker AVANCE 400 MHz spectrometer (Bruker) with a 5 mm BBFO probe using deuterated dimethylsulfoxide (DMSO-d₆) as the solvent (Germany). Molecular weight was determined by Gel Permeation Chromatography type; Agilent 1100, Germany. The measurements were conducted at ambient temperature using dimethylformamide (DMF) and H₂O as the mobile phase at a flow rate of 1.0 ml/ min. High molecular weight (P1) was dissolved in DMF, while low molecular weight polymer (P2) was dissolved in H₂O as the mobile phase at a concentration of 5mg/ml and the amount of each injected sample was 100 μ l. Polystyrene standards with a concentration of 1mg/ml were used for calibration (molecular weight as follows: 393.4k, 233.2k, 114.4k, 44.1k, 13.2k, 3.68, 2.33k, and 820). The calibration curve was plotted with the logarithm of average molecular weight as a function of elution volume. Morphological studies have been measured using a scanning electron microscope (SEM) (JEOL JXA- 840 A Electron PROBE, Japan), a micro-analyzer microscope (Japan).

2.3. Synthesis of 2-Amino-4-(1-benzyl-1H-indol-3-yl) thiophene-3-carbonitrile synthesis (ABITC)

ABITC was prepared as reported by El-Sawy coworkers [13]. Melting point, color, and the spectral data of ABITC were in agreement with the previously reported data.

2.4. Preparation of poly (2-amino-4-(1-benzyl-1H-indol-3-yl) thiophene-3-carbonitrile) (PABITC):

To an emulsifier solution of ammonium persulfate (2g) and sodium dodecylbenzene sulfonate (SDBS) (0.005 gm) in distilled water (70ml), 2-amino-4-(1-benzyl-1H-indol-3-yl) thiophene-3-carbonitrile (0.3g) in ethanol (20ml) was added drop-wise under stirring at room temperature. The reaction mixture was kept under stirring for 24h until polymerization was completed. The formed precipitate was filtered off afforded the first isomer (high molecular weight

polymer, P1). The filtrate was poured into ethanol (100 ml) and stirred for another 2h, then the formed precipitate was filtered off, washed several times and dried at 60°C for 24h to obtain the second isomer (low molecular weight polymer, P2).

2.5. General procedure for Preparation of Nano-Capsules

PEG-based nanoparticles were synthesized using precipitation method[15]. Tween 80, (SDS), macrogol 6000 (PEG), sodium carboxymethyl cellulose (SCMC), sodium carboxy methyl dextran (SCMD), and/or doxorubicin (DOX) were used as excipients. Each excipient (0.01, 0.03, 0.05, 0.1, and 0.004 g; respectively) was dissolved in 1 mL distilled water.

2.6. Preparation of (ABITC, P 1 and P2)/ PEG-Nanoparticles

Solutions of the ABITC, P1, and P2 in ethanol (0.004 g/ 1 mL) were added drop by drop to the aqueous solutions of excipients (Tween 80, SDS, macrogol 6000 (PEG), SCMC and SCMD) under stirring at 600 rpm. After the addition was completed, the stirring was continued for a further 10 min at 35°C (600 rpm). The mixtures were vortexed for 5 min and subsequently sonicated for 5 min using a Sonics Vibra-cell sonifier VC750 equipped with a micro-tip (Newtown, CT) at amplitude = 35%, pulse-on = 5.0 s, and pulse-off = 3.0 s. Finally, the suspensions transferred to a round-bottom tube in a water bath with magnetic stirring overnight at room temperature.

2.7. Preparation of DOX-loaded (P1 and P2)/ PEG-Nanoparticles

A solution of the P1 and P2 in ethanol (0.004 g/ 1 mL) was slowly dropped to the aqueous solutions of excipients (Tween 80, SDS, macrogol 6000 (PEG), SCMC, SCMD, and DOX) under stirring at 600 rpm. The system keeps stirred at 600 rpm for 10 min at 35°C. Then the mixtures were vortexed for 5 min and subsequently sonicated for 5 min using a Sonics Vibra-

cell sonifier VC750 equipped with a micro-tip (Newtown, CT) at amplitude = 35%, pulse-on = 5.0 s, and pulse-off = 3.0 s. Finally, the suspensions transferred to a round-bottom tube in a water bath with magnetic stirring overnight at room temperature.

2.8. Biological assay

2.8.1. In-vitro studies (Cell culture and maintenance)

Human hepatocellular carcinoma cell lines (HepG2 and Huh-7) and non-small cell lung cancer (A549) were purchased from VASCERA Co. (Vaccines Sera and Drugs) supplied them from American Type Culture Collection (ATCC, USA). Lung and liver cells were cultured using Dulbecco's modified Eagle's medium (DMEM) and Roswell Park Memorial Institute (RPMI-1640) medium. All media were supplemented with 4.5 g/L Glucose with L-Glutamine and 10% fetal bovine serum (FBS). The cells were incubated in 5% CO₂ humidified at 37°C for growth maintenance.

2.8.2. MTT cytotoxicity assay

Cell viability was studied using the MTT 3-(4,5-dimethylthiazol-2-yl)-2,5-diphenyl-tetrazolium bromide assay[20]. Briefly, the cells were cultured in 96-well plates at a density of 1×10^4 cells/well. All formulations with their described concentrations (0, 25, 50, 75, and 100 µg/mL) were added in the media over these cell lines. Culture media with nano-void (i.e. nano-capsule without loaded drug) and without were added as controls for the drug-loaded nano-formulations and their free counterparts. After 24 h incubation, MTT dissolved in PBS was added to each well at a final concentration of 5 mg/ml, and the samples were incubated at 37°C for 4 h. Water-insoluble dark blue formazan crystals that formed during MTT cleavage in actively metabolizing cells

were then dissolved in dimethyl sulfoxide (DMSO). Absorbance was measured at A_{540} nm, using a microplate reader (BMG Labtech, Germany). The cell viability (%) was calculated and compared with the controls.

2.8.3. Antimicrobial evaluation

The antimicrobial activity of the synthesized compounds was evaluated in vitro using agar well diffusion method [21] against four different pathogenic microorganisms: *Bacillus subtilis* (ATCC 35854), *Staphylococcus aureus* (ATCC 25923) (Gram-positive bacteria), *Escherichia coli* (ATCC25922) and *Pseudomonas aeruginosa* (ATCC 9027) (Gram-negative bacteria). The microbial strains were obtained from the culture collection of Microbiological Resources Centre (MIRCEN), Faculty of Agriculture, Ain Shams University, Cairo, Egypt. Muller Hinton liquid and solid media (Sigma) were sterilized at 121 °C for 20 min then used for subculture and assay by the agar-well diffusion method. Dimethyl sulfoxide (DMSO) was used as a solvent for impregnation. Amikacin was used as reference drugs.

Muller Hinton agar (25 mL) was seeded with the tested bacterial culture (25 ul) and then poured into sterile Petri dishes (10 mL) and allowed to solidify. Wells of 8 mm diameter were punched aseptically with a sterile cork borer and 200 ul of the tested compounds (20 mg/ml in DMSO 1.5%) was introduced into each well. The plates were left for 30 min at room temperature to allow the diffusion of each substance. The agar plates were incubated at 37 °C for 24 h and the inhibition zones (IZ) were measured. The experiment was performed in triplicate, and the average zone of inhibition was calculated.

2.9. In Silico Molecular Docking Study

The mode of interaction of the monomer ABITC and two repeated unite of monomer (ABITC)₂ were studied theoretically by molecular docking technique using the MOE program (Molecular Operating Environment, 2008.10) against two different biological targets. The biological targets including the crystal structures of DNA gyrase B chain in complex with Novobiocin (PDB ID: 1KIJ)[22] as promising bacterial target and Crystal structure of CDK2 in complex with PM1 [2-amino-6-(2,6-difluorobenzoyl)-imidazo[1,2-a]pyridin-3-yl]-phenyl-methanone (PDB ID: 1PYE)] [23] as promising cancer target were downloaded from a protein data bank (<https://www.rcsb.org>) and prepared for docking process. To validate the docking protocol, the co-crystalline ligands Novobiocin and PM1 were docked in the active site of 1KIJ and 1PYE, respectively. 2D structures of ABITC and (ABITC)₂ were drawn in ChemDraw Ultra 12.0 then converted to 3D and minimized using the MMFF94x force field to 0.01 Kcal mol⁻¹Å⁻¹ [24]. MOE-DOCK default was used to posing the molecule into the active site (Algorithm).

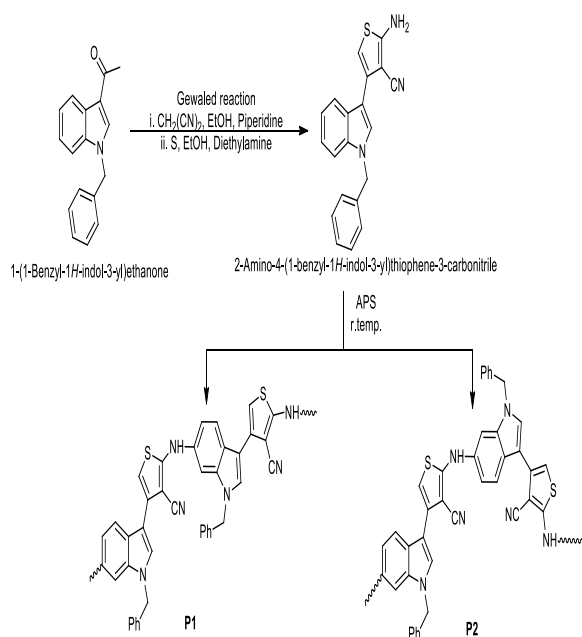
2.10. Statistical analysis

All assays were repeated three independent times (n=3). Comparisons between nano-formulations and their free counterparts versus controls were made using a two-tailed Student's t-test, and values of P < 0.05 were considered statistically significant.

3. Results and discussion

3.1. Polymerization

The general synthetic route for the synthesis of ABITC, P1, and P2 is outlined in Scheme 1. First, 2-amino-4-(1-benzyl-1H-indol-3-yl) thiophene-3-carbonitrile (ABITC) was prepared via Gewald reaction which undergo emulsion polymerization afforded the corresponding poly(2-amino-4-(1-benzyl-1H-indol-3-yl) thiophene-3-carbonitrile). From literature, we found that ethanol can act as a meta-stabilizer for spherical micelles under stirring [25]. Sundburg reported that reactivity of indole ring follows the trend $3 > 2 > 6 > 4 > 5 > 7$ [26]. Also, the electrochemical synthesis of poly (indole-co-thiophene) was studied by Gopi and his coworkers which in agreement with Sundberg reactivity order [27]. As a result of all these findings, we propose the mechanism for the ABITC polymerization as depicted in **Scheme 1** assisted by FTIR and $^1\text{H-NMR}$ spectral data. The polymerization was achieved through the thiophene amino group and the C6 of indole moiety.



Scheme 1: Synthesis and polymerization of (2-amino-4-(1-benzyl-1H-indol-3-yl) thiophene-3-carbonitrile)

$^1\text{H-NMR}$ revealed three singlet signals at 8.56, 8.2, 7.52, and 5.50 related to indolyl H-2, thienyl H-5, NH, and CH_2 groups, respectively. Besides multiple signals at the chemical shift ranging from 7.37 to

7.20 for only 9 aromatic protons lack the proton of C6 according to literature protons of C4, C5 and C7 appeared at 7.52, 7.02, 7.3 respectively [28] (**Figure 1**).

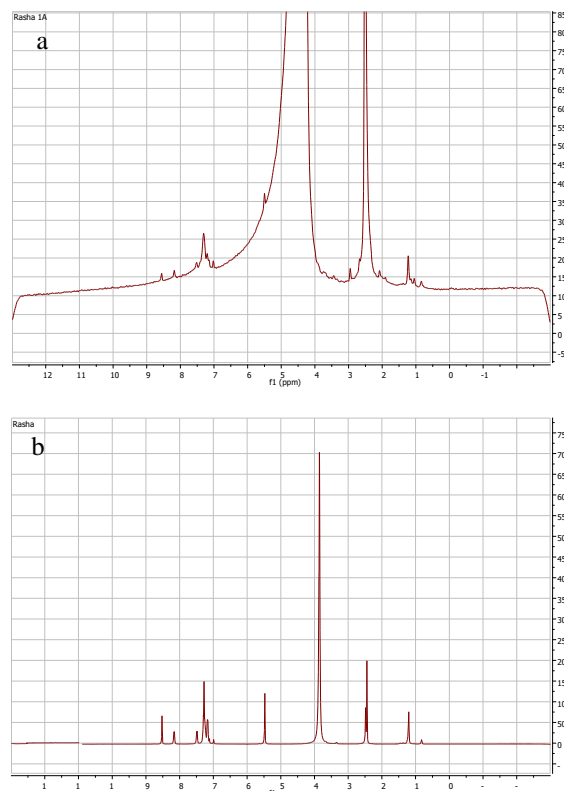


Figure 1: $^1\text{H-NMR}$ of polymer (a) P1 and (b) P2

While, FTIR spectrum of polymers PABITC revealed two bands at 3401 and 3103cm^{-1} related to the NH group of P1 and P2 respectively. Besides peaks at 2278 , 1636 , 1462 , 1384 , and 742cm^{-1} related cyano, $\text{C}=\text{C}$, benzenoid rings, $\text{C}-\text{N}$, and $\text{C}-\text{S}$ groups, respectively (**Figure 2**).

The gel permeation chromatography (GPC) was used to determine the weight-average molecular weights (M_w) of the new polymers. GPC revealed that the M_w of the P1 is 35673 g/mol with PDI (polydispersity index, M_w/M_n) 1.19, and P2 is 28596 with PDI (polydispersity index, M_w/M_n) value of 1.21.

The optical properties of ABITC, P1, and P2 solutions (DMSO were used as solvent) were determined using UV-vis spectroscopy (Figure 3). The UV-vis result showed that each of ABITC, P1, and P2 have three absorption peaks and ABITC, P2 showed a slight redshift compared to P1. Monomer ABITC revealed peaks at 245nm , 389nm , and

429nm. While, P1 showed absorption peaks at 245nm, 388nm, 413nm, and 487nm. Furthermore, P2 showed peaks at 245nm, 324nm, 362nm (Table 1).

The morphology structure of the P1 and P2 was studied using Scanning Electron Microscope SEM **Figure 4**. The SEM result indicated that the P1 structure was smooth flakes where P2 showed rod structure.

Moreover, the solubility result of the newly synthesized polymers showed that P1 and P2 had good solubility in different polar solvents at room temperature such as dimethylformamide (DMF), tetra hydro furan (THF), dimethyl sulfoxide (DMSO), chloroform and H₂O except P1 was insoluble in H₂O at room temperature and complete solubility at 60°C as shown in **Table 1**.

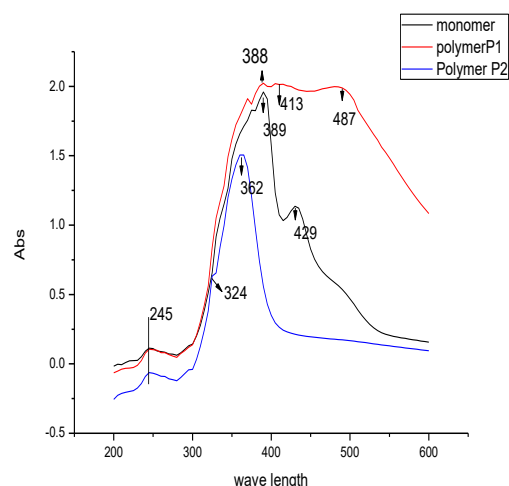


Figure 3: UV-vis of polymers (P1, P2) in comparison to monomer in DMSO

3.2. Nano-capsulation

The average size distribution, zeta potential, and polydispersity index (PDI) of the synthesized nanoparticles were shown in **Table 2**. Nano-formulation of ABITC-PEG-NP had the lowest average nano-size with good stability and low PDI. The P1-PEG-NP, DOX P1-PEG-NP, P2- PEG-NP and DOX P2- PEG-NP nano-formulations were very stable with negatively charged zeta potential on their surfaces and very low PDI records. The lower number of PDI below 0.5 confirmed the results of zeta potential, which indicates that our nanoformulations were very stable.

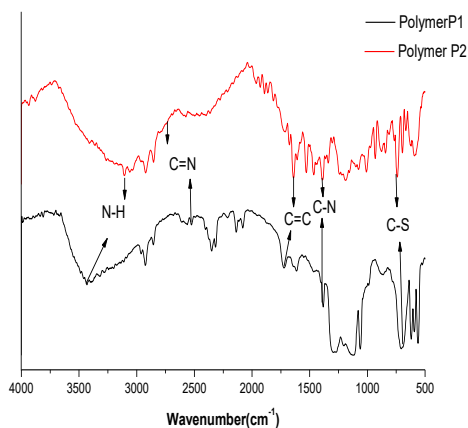


Figure 2: FTIR spectrum of polymer P1 and P2

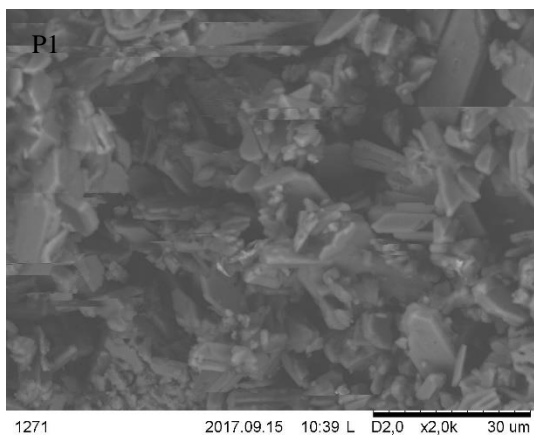


Figure 4: The SEM morphology structure of the polymer P1 and polymer P2

Table 1: Solubility of polymer P1 and P2 in different solvents

solvents	Polymer P1	Polymer P2
H ₂ O	Insoluble at room temp. but completely soluble at 60°C	Completely soluble
Dimethylformamide (DMF)	partial soluble	Completely soluble
Tetra hydro furan (THF)	partial soluble	Completely soluble
Dimethyl sulfoxide (DMSO)	Completely soluble	Completely soluble
Chloroform	Completely soluble	Completely soluble
Toluene	Partial soluble	Partial soluble
n-Heptane	Insoluble	Insoluble

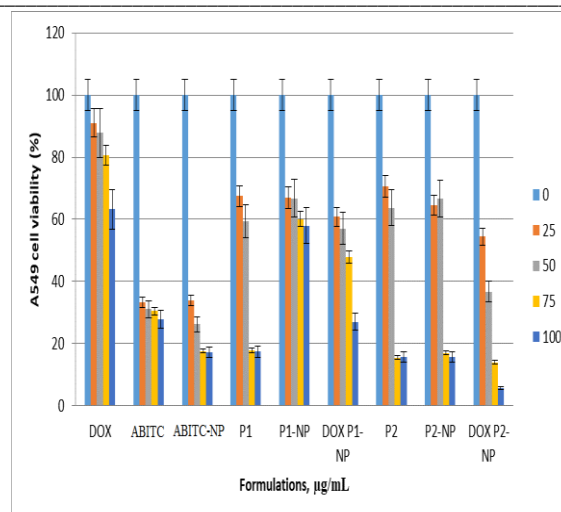


Figure 5: The anti-proliferative effects of the synthesized formulations against A549 lung cancer cell line.

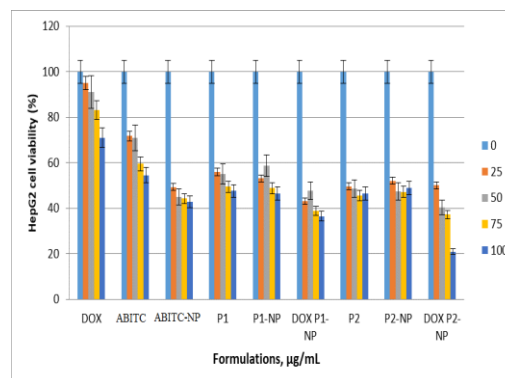


Figure 6: The anti-proliferative effects of the synthesized formulations against HepG2 liver cancer cell line

Table 2: Average of size, PDI, and Zeta potential of ABITC, P1, and P2 nanoparticles.

NPs type	Size, nm	PDI	Zeta, mV
ABITC-PEG-NP	151.6 +6.4	0.01 +0.00	-15.5 +3.2
P1- PEG-NP	275.8 +4.5	0.02 +0.00	-12.1 +1.0
DOX P1- PEG-NP	296.7 +7.4	0.01 +0.00	-9.7 +0.5
P2- PEG-NP	292.5+7.3	0.05 +0.00	-13.6+2.5
DOX P2- PEG-NP	302.2+13.8	0.1 +0.0	-7.2+1.1

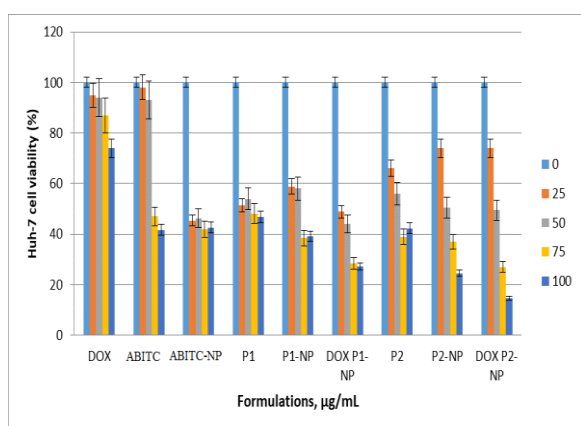


Figure 7: The anti-proliferative effects of the synthesized formulations against Huh-7 liver cancer cell line.

3.3. Biological activity

3.3.1. Anti-cancer activity

The anti-proliferative activity of the free monomer (ABITC) and two polymers (P1, P2) beside their nano-encapsulation were screened against human liver cancer (HepG2 & Huh7) and human lung cancer (A549) using MTT assay (Table 3). Also, the impact of loading doxorubicin (DOX) as a positive standard anticancer control was studied. The IC₅₀ of DOX was undetectable (> 100 µg/ml) upon human lung cancer A549 cells as well as human liver cancer HepG2 and Huh-7 cells. The results obtained indicate that all free and nano-formulations showed a significant gradual

decrease ($P < 0.05$) upon A549, HepG2, and Huh-7 cancer cell lines (Figure 5-7). The free monomer ABITC showed moderate anti-proliferative activity against A549 and Huh-7 cancer cell lines with IC₅₀ value 24.96, 87.44 µg/ml, respectively while there was not detected IC₅₀ upon HepG2 cancer cells.

Encapsulate ABITC inside PEG-NP result in improving their anti-proliferative activity with the IC₅₀ 23.58, 34.96, and 36.77 µg/ml against HepG2, Huh-7 and HepG2 cancer cell lines with the fold changed equal 1.05, 2.5 and 2.71-time, respectively compared to free ABITC (Table 3). While, polymer P1 showed moderate anti-proliferative activity against A549, HepG2, and Huh-7 cells with IC₅₀ value of 47.79, 50.48, and 45.26 µg/ml, respectively. Encapsulation of P1 in PEG-NP revealed no significant change in the activities and the fold changes were as follows: 0.47, 0.96, and 0.91 (i.e. not exceed 1-time fold compared to free P1). Furthermore, the IC₅₀s of P1-NP was improved (lowered in their number and the anticancer activity increased) after DOX encapsulation as follow: 56.67, 34.85 and 34.25 µg/ml, with fold, changed equal 1.76, 1.49 and 1.44 against A549, HepG2, and Huh-7 cells, respectively compared to P1- PEG-NP and this overcome the DOX resistance among the tested cancer cell lines (Table 3). On the other hand, P2 showed moderate anti-proliferative activity against A549, HepG2, and Huh-7 cancer cell lines with IC₅₀ value 50.61, 38.97, and 51.85 µg/ml, respectively. Encapsulation of P2 in PEG-NP showed no significant changed in the anti-

proliferative activity against HepG2 and Huh-7 cell lines, the fold changes were 0.98 (i.e. not exceed 1 time fold compared to free (P2), while against A549 cells the fold change was 1.002. Moreover, The IC50s of P2-NP was improved after DOX encapsulation as follow: 33.10, 36.37 and 48.64 $\mu\text{g/ml}$, with fold, changed equal 1.52, 1.08, and 1.07 against A549, HepG2, and Huh-7 cells, respectively compared to P2-PEG-NP and this overcome the DOX resistance among the tested cancer cell lines (Table 3).

3.3.2. Anti-bacterial activity

A previous study revealed that the monomer ABITC was inactivity against a variety of pathogenic microorganisms such as *B. subtilis*, *S. aureus*, and *S. typhimurium* [13]. In the present work, the antimicrobial activity of the newly synthesized polymers only was evaluated in vitro using agar well diffusion method against four different pathogenic microorganisms: *B. subtilis* (ATCC 35854), *S. aureus* (ATCC 25923) (Gram-positive bacteria), *E. coli* (ATCC25922) and *P. aeruginosa* (ATCC 9027) (Gram-negative bacteria) comparing to Amikacin as reference drug which is a broad spectrum antibiotic against gram negative organisms such as *E. coli* and *P. aeruginosa* beside some gram positive organisms such as *B. subtilis* and *S. aureus*. The data obtained showed that the new polymers P1 and P2 exhibited potent antibacterial activity comparing to monomer ABITC and this may be due to the long chain of the polymer, which means the repeating of the active groups. Polymer P1 showed moderate activity against *S. aureus* and *B. subtilis* with inhibition zones 22 and 18.5 mm compared to the reference drug amikacin of 30 and 21mm, respectively (Table 4). Whereas, P1 exhibited potent activity against *E. coli* and *P. aeruginosa* with inhibition zones 15.5 and 19 mm greater than the reference drug amikacin of 15 & 18 mm, respectively. Furthermore, P2 showed potent

activity against only *Pseudomonas aeruginosa* with an inhibition zone of 19mm higher than amikacin of 18 mm (Table 4)

3.4. In Silico Molecular Docking Study

From biological results, we found that the polymers P1 and/or P2 have better activity than the monomer, especially in antibacterial evaluation. Hence, the docking study was carried out to identify the mode of interaction of the monomer ABITC beside two repeated units of monomer (ABITC)₂ to clarify if using more than one monomer unit will improve the docking result as well as the biological result. The docking studies were conducted against the active site of DNA gyrase B chain in complex with Novobiocin (PDB ID: 1KIJ) as promising bacterial target and CDK2 enzyme in complex with PM1 (PDB ID: 1PYE) as promising cancer target using program MOE 2008.10.

3.4.1. Docking study against DNA gyrase B chain

DNA gyrases are well-studied drug targets present in nearly all bacteria and are important for bacterial growth [29, 30]. The weak structural homology with human topoisomerases that these enzymes show makes them ideal targets for antibacterial therapy. These enzymes are often composed of two subunits. The DNA gyrase (GyrB) B-subunit is made up of ATP binding pockets that are responsible for the replication of DNA. The inhibition of this pocket by small molecules is possible, and several lead compounds have been produced by targeting this pocket [31, 32]. The docking result revealed that monomer ABITC exhibited a good docking score of -19.80 kJ/mol, Compared to Novobiocin of -24.40 and Rmsd 2.23 (Table 5). Also, ABITC showed effective fitting inside the protein active pocket via the creation of

hydrogen bond with the same amino acid residue (Arg 75) as Novobiocin beside hydrogen bond between NH₂ group and amino acid residue Glu 49 (**Table 5, Fig 8-9**). While two repeated units of monomer (ABITC)₂ revealed docking score of -25.19 kJ/mol, better than Novobiocin and ABITC of -24.40 and -19.80 kJ/mol, respectively. Moreover (ABITC)₂ exhibited better fitting inside the protein active pocket via creation of hydrogen bonds with the same amino acid residue (Arg 135) as Novobiocin beside hydrogen bond (NH₂ group with Glu 136) and Arene-cation interaction between benzyl ring and amino acid residue Lys 109 (**Table 5, Fig 10**).

3.4.2. Docking study CDK2 enzyme (PDB ID: 1PYE)

Cyclin-dependent kinase 2 (CDK2), also known as cell division kinase, one of the serine/threonine kinase family that plays a vital role in controlling the cell cycle, such as propagation, division, neuronal activity and apoptosis [33, 34, 35]. CDK2's over-expression will result in massive types of cancer such as colorectal, lung, pancreatic and liver cancer, etc [36]. Several CDK2 inhibitors were identified based on privileged scaffolds such as indoles, pyridines, pyrimidines, thiazoles, etc [37, 38, 39, 40].

The docking result obtained showed that monomer ABITC exhibited a good docking score of -19.80 kJ/mol, equal to PM1 of -19.80 kJ/mol and RMSD 1.60 (Table 5). Also, ABITC showed good fitting inside the protein active site via the formation of two donating hydrogen bonds between the NH₂ group with amino acid residues Asn 132 and Asp 145 compared to PM1 with only one hydrogen bond (Table 5, Fig 11-12). While two repeated units of monomer (ABITC)₂ revealed a docking score of -31.74kJ/mol, higher than PM1 and ABITC of -19.80 kJ/mol. (ABITC)₂ exhibited better fitting inside the protein active pocket

via the creation of one hydrogen bond (NH₂ group with ASN 132) and Arene-cation interaction between Indole moiety and amino acid residue Lys 129 (Table 5, Fig 13).

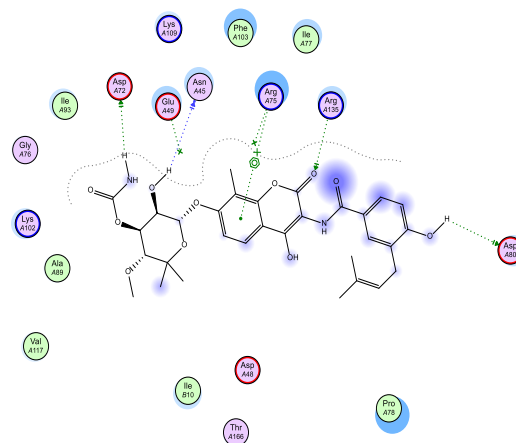


Figure 8a: The 2D binding mode of Novobiocin into the active site of DNA gyrase B chain (PDB ID: 1KIJ).

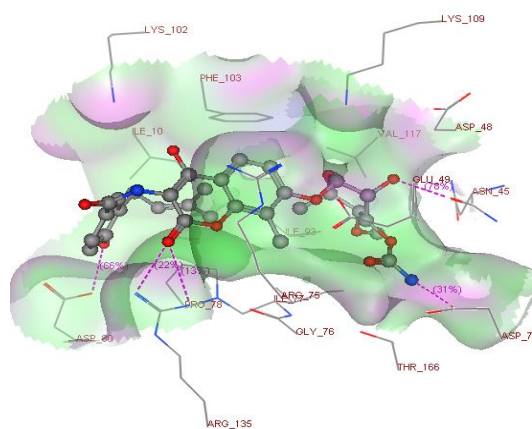


Figure 8b: The 3D binding mode of Novobiocin into the active site of DNA gyrase B chain (PDB ID: 1KIJ).

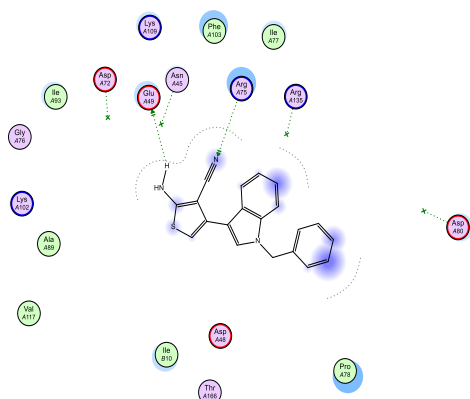


Figure 9a: The 2D binding mode of ABTC into the active site of DNA gyrase B chain (PDB ID: 1KIJ).

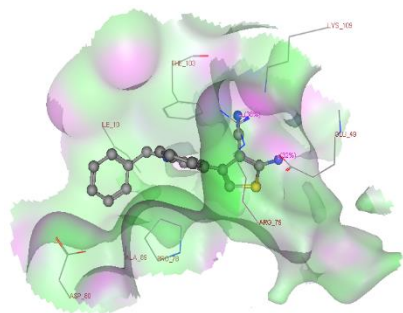


Figure 9b: The 3D binding mode of ABTC into the active site of DNA gyrase B chain (PDB ID: 1KIJ).

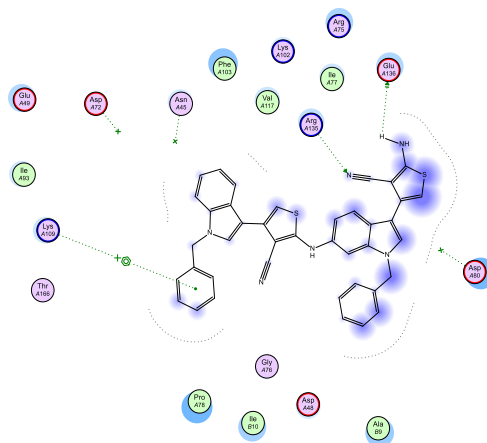


Figure 10a: The 2D binding mode of (ABITC)₂ into the active site of DNA gyrase B chain (PDB ID: 1KIJ)

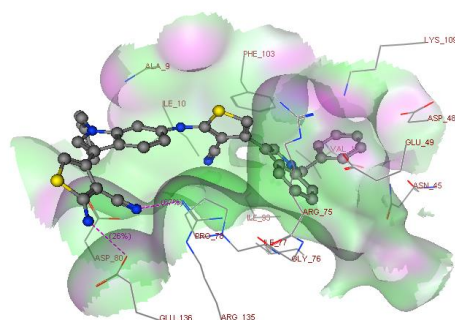


Figure 10b: The 3D binding mode of (ABITC)₂ into the active site of DNA gyrase B chain (PDB ID: 1KIJ)

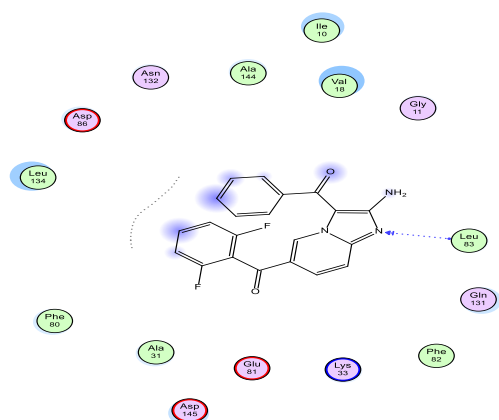


Figure 11a: The 2D binding mode of PM1 into the active site of CDK2 enzyme (PDB ID: 1PYE)

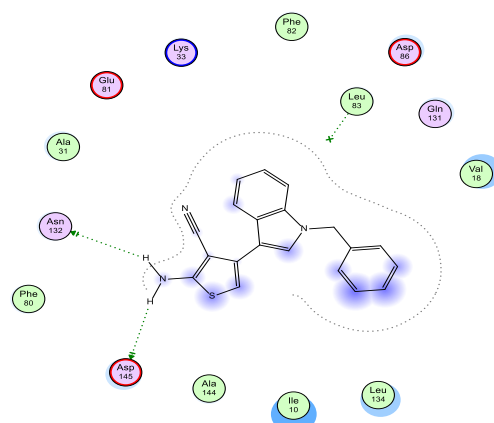


Figure 12a: The 2D binding mode of ABTC into the active site of CDK2 enzyme (PDB ID: 1PYE)

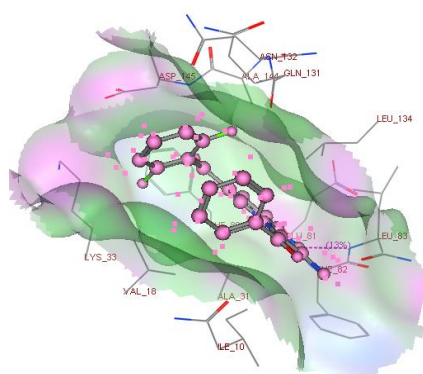


Figure 11b: The 3D binding mode of PM1 into the active site of CDK2 enzyme (PDB ID: 1PYE)

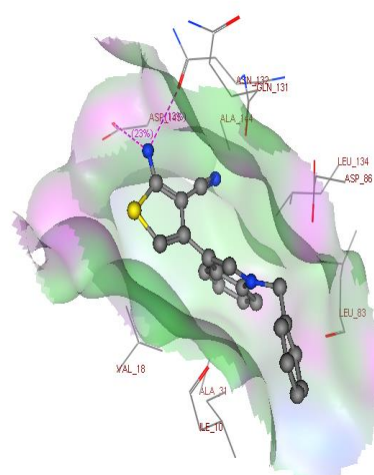


Figure 12b: The 3D binding mode of ABTC into the active site of CDK2 enzyme (PDB ID: 1PYE)

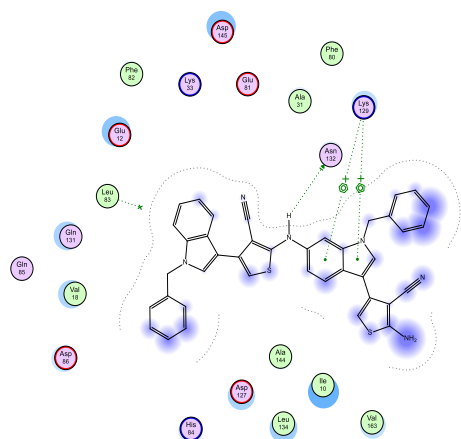


Figure 13a: The 2D binding mode of (ABITC)2 into the active site of CDK2 enzyme (PDB ID: 1PYE)

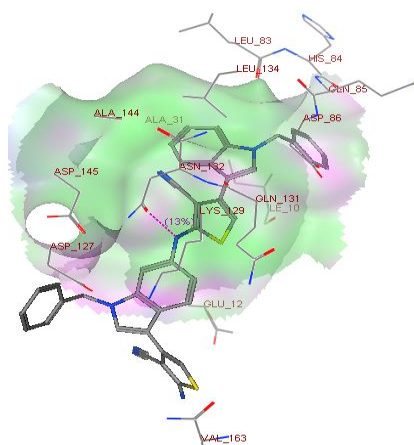


Figure 13b: The 3D binding mode of (ABITC)2 into the active site of CDK2 enzyme (PDB ID: 1PYE)

Table 3: IC50 and the fold change for ABITC, P1, P2, and their nano-encapsulated counterparts against A549 (human lung cancer cells), HepG2 and Huh-7 (human hepatocellular carcinoma cells).

Samples	A549		HepG2		Huh-7	
	IC50 $\mu\text{g/mL}$	Fold change	IC50 $\mu\text{g/mL}$	Fold change	IC50 $\mu\text{g/mL}$	Fold change
DOX	> 100	-	> 100	-	> 100	-
ABITC	24.9664	Ref	> 100	Ref	87.44063	Ref
ABITC-PEG-NP	23.58658	1.058501*	36.77942	2.718912**	34.96879	2.500533**
P1	47.79683	Ref	50.48118	Ref	45.26898	Ref
P1- PEG-NP	> 100	0.477968	52.06984	0.96949	49.39293	0.916507
DOX P1- PEG-NP	56.67496	1.764448*	34.85976	1.493695*	34.25117	1.44208*
P2	50.6195	Ref	38.97711	Ref	51.85269	Ref
P2- PEG-NP	50.48878	1.002589	39.54444	0.985653	52.5248	0.987204
DOX P2- PEG-NP	33.10155	1.525269*	36.37585	1.087107*	48.64718	1.079709*

DOX was used as a positive anticancer agent; > 100 means undetectable IC50; Fold change was calculated by dividing the free drug by the nano-encapsulated counterpart. When the fold change is higher than 1, it represents that the nano-encapsulated agent is more effective against cancer cells than its free counterpart.; Ref. means taking the free agent as a reference to its nano-encapsulated counterpart.

T test were performed using SPSS

* means significant difference (p less than 0.5) when compared treatment with the reference

** means high sig difference (p less than 0.01) when compared treatment with reference

Table 4: the antimicrobial activity of ABITC, P1, and P2 (20 mg/disc). a

Samples b	Inhibition zone (mm) c			
	Gram-Positive		Gram-Negative	
	S. Aureus (ATCC 25923)	B. Subtilis (ATCC 35854),	E. Coli (ATCC25922)	P. Aeruginosa (ATCC 9027)
P1	22	18.5	15.5	20.5
P2	10	NA	NA	19
ABITC	NA	NA	NA	NA
DMSO	10	NA	10	10
Amikacin	30	21	15	18

a disk diffusion method; b concentration 20 μg ; c each value is the mean of three values; DMSO: Dimethylsulfoxide; NA mean is unactive

Table 5: Docking results of the monomer ABTC and two repeated units of monomer (ABITC)₂ into the active site of DNA gyrase B chain (PDB ID: 1KIJ) as promising bacterial target and CDK2 enzyme (PDB ID: 1PYE) as a promising cancer target

Compounds No.	Binding Energy (kJ mol ⁻¹)	Main atoms from the compounds	Amino acid residue	Type of interaction and bond length (Å)
DNA gyrase B chain(PDB ID: 1KIJ)				
Novobiocin	-24.40 Rmsd: 2.23	Hydrogen atom of OH group	Asn 45	H-don (1.79)
		Hydrogen atom of NH ₂ group	Asp 72	H-don (1.87)
		Oxygen atom of CO group	Arg 135	H-acc (2.86)
		Hydrogen atom of OH group	Asp 80	H-don (1.84)
		Benzene ring	Arg 75	Arene-Cation
ABTC	-19.80	Hydrogen atom of NH ₂ group	Glu 49	H-don (1.62)
		Nitrogen atom of CN group	Arg 75	H-acc (2.89)
(ABITC) ₂	-25.19	Hydrogen atom of NH ₂ group	Glu 136	H-don (1.70)
		Nitrogen atom of CN group	Arg 135	H-acc (2.72)
		Benzyl ring	Lys 109	Arene-cation
CDK2 enzyme (PDB ID: 1PYE) CDK2 enzyme (PDB ID: 1PYE)				
PM1	-20.06 Rmsd: 1.60	N 4384 N 1122 1PYE 1	Leu 83	H-acc (3.07)
ABTC	-19.80	Hydrogen atom of NH ₂ group	Asn 132	H-don (1.73)
		Hydrogen atom of NH ₂ group	Asp 145	H-don (1.63)
(ABITC) ₂	-31.74	Hydrogen atom of NH group	ASN 132	H-don (1.99)
		Indole moiety	Lys 129	Arene-Cation

4. Conclusion

Two bioactive isomers of poly (2-amino-4-(1-benzyl-1H-indol-3-yl) thiophene-3-carbonitrile) (PABITC) with high molecular weight 35673 and 28596 g/mol were synthesized via emulsion polymerization. The new polymer P1 exhibited potent activity against *Escherichia coli* and *Pseudomonas aeruginosa* with inhibition zones 15.5 and 19 mm greater than the reference drug amikacin of 15 & 18 mm, respectively. While P2 showed potent activity against *Pseudomonas aeruginosa* with an inhibition zone of 19mm higher than amikacin of 18 mm. Nano-capsulation of ABITC, PABITC, and PABITC/Doxorubicin (DOX) by polyethylene glycol (PEG) was achieved by nano-precipitation method. The anti-proliferative activity of P1-NP and P2-NP were improved after DOX encapsulation with IC₅₀ value ranging from 56.67 to 33.10µg/ml against A549, HepG2, and Huh-7 cells

with the fold changed ranging from 1.76 to 1.07 compared to P1- PEG-NP and P2- PEG-NP. The mode of interaction of ABITC and (ABITC)₂ was studied by molecular docking technique. (ABITC)₂ revealed better docking score beside good fitting inside the active site of both DNA gyrase B chain and CDK2 enzymes than ABITC and this was in agreement with biological.

Authors Contribution

Rasha A. Baseer conceived of the main idea, carried out the polymerization experiment, managed the experiment process, and wrote the manuscript with support from Ahmed A. Abd-Rabou and H. M. Abo-Salem.

H. M. Abo-Salem synthesized the monomer and carried out the molecular docking studies.

Ahmed A. Abd-Rabou prepared nano-capsules in addition to performing Biological assay and MTT cytotoxicity assay.

Rasha A.M Azouz performed antimicrobial studies and wrote its experimental part.

Eman S. Zarie assisted with HNMR, FT-IR, and SEM analysis which was carried out in Nano-chemistry and Nano-engineering, School of Chemical Technology, Aalto University.

Acknowledgment

The authors are thankful to Nano-chemistry and Nano-engineering, School of Chemical Technology, Aalto University for their fruitful cooperation and assistance in carrying out some necessary analyzes.

Conflict of interest

The authors declare there is no conflict of interest, financial, or otherwise.

References

1. Organization W.H. Cancer. 2018; Available from: <http://www.who.int/en/news-room/fact-sheets/detail/cancer>
2. Padma V.V., (2015) An overview of targeted cancer therapy. *BioMedicine*. 5(4): p. 19-19.
3. Bajpai A.K., Shukla S.K., Bhanu S.,Kankane S., (2008) Responsive polymers in controlled drug delivery. *Progress in Polymer Science*. 33(11): p. 1088-1118.
4. Cambón A., Rey-Rico A., Mistry D., Brea J., Loza M., Attwood D., Barbosa S., Alvarez-Lorenzo C., Concheiro A.,Taboada P., (2013) Doxorubicin-loaded micelles of reverse poly (butylene oxide)–poly (ethylene oxide)–poly (butylene oxide) block copolymers as efficient “active” chemotherapeutic agents. *International journal of pharmaceutics*. 445(1-2): p. 47-57.
5. Rasolonjatovo B., Gomez J.-P., Mème W., Gonçalves C., Huin C.c., Bennevault-Celton V.r., Le Gall T., Montier T., Lehn P.,Cheradame H., (2015) Poly (2-methyl-2-oxazoline)-b-poly (tetrahydrofuran)-b-poly (2-methyl-2-oxazoline) amphiphilic triblock copolymers: synthesis, physicochemical characterizations, and hydrosolubilizing properties. *Biomacromolecules*. 16(3): p. 748-756.
6. Li H.,Niu Y., (2018) Synthesis and characterization of amphiphilic block polymer poly (ethylene glycol)-poly (propylene carbonate)-poly (ethylene glycol) for drug delivery. *Materials Science and Engineering: C*. 89: p. 160-165.
7. Bae J., Maurya A., Shariat-Madar Z., Murthy S.N.,Jo S., (2015) Novel redox-responsive amphiphilic copolymer micelles for drug delivery: Synthesis and characterization. *The AAPS journal*. 17(6): p. 1357-1368.
8. Yan J., Ye Z., Chen M., Liu Z., Xiao Y., Zhang Y., Zhou Y., Tan W.,Lang M., (2011) Fine tuning micellar core-forming block of poly (ethylene glycol)-block-poly (ϵ -caprolactone) amphiphilic copolymers based on chemical modification for the solubilization and delivery of doxorubicin. *Biomacromolecules*. 12(7): p. 2562-2572.
9. Vaculikova E., Grunwaldova V., Kral V., Dohnal J.,Jampilek J., (2012) Primary investigation of the preparation of nanoparticles by precipitation. *Molecules*. 17(9): p. 11067-11078.
10. Abd-Rabou A.A.,Ahmed H.H., (2017) CS-PEG decorated PLGA nano-prototype for delivery of bioactive compounds: A novel approach for induction of apoptosis in HepG2 cell line. *Advances in medical sciences*. 62(2): p. 357-367.
11. Ahmed H.H., Galal A.F., Shalby A.B., Abd-Rabou A.A.,Mehaya F.M., (2018) Improving anti-cancer potentiality and bioavailability of gallic acid by designing polymeric nanocomposite formulation.

- Asian Pacific journal of cancer prevention: APJCP. 19(11): p. 3137.
12. McGarry D.H., Cooper I.R., Walker R., Warrilow C.E., Pichowicz M., Ratcliffe A.J., Salisbury A.-M., Savage V.J., Moyo E., Maclean J., (2018) Design, synthesis and antibacterial properties of pyrimido [4, 5-b] indol-8-amine inhibitors of DNA gyrase. *Bioorganic & medicinal chemistry letters*. 28(17): p. 2998-3003.
13. El-Sawy E., Mandour A., Mahmoud N., Abo-Salem H., (2012) Some new 2-amino-4-(N-substituted-1H-indol-3-yl) thiophene-3-carbonitriles and their antimicrobial properties. *Egypt J Chem*. 55.
14. Lee C.M., Choi Y.J., Park S.-H., Nam M.J., (2018) Indole-3-carbinol induces apoptosis in human hepatocellular carcinoma Huh-7 cells. *Food and chemical toxicology*. 118: p. 119-130.
15. Dulla B., Sailaja E., CH U.R., Aeluri M., Kalle A.M., Bhavani S., Rambabu D., Rao M.B., Pal M., (2014) Synthesis of indole based novel small molecules and their in vitro anti-proliferative effects on various cancer cell lines. *Tetrahedron Letters*. 55(4): p. 921-926.
16. Fouad M.M., El-Bendary E.R., Shehata I.A., El-Kerdawy M.M., (2018) Synthesis and in vitro antitumor evaluation of some new thiophenes and thieno [2, 3-d] pyrimidine derivatives. *Bioorganic chemistry*. 81: p. 587-598.
17. Mohareb R.M., Abdallah A.E.M., Mohamed A.A., (2018) Synthesis of novel thiophene, thiazole and coumarin derivatives based on benzimidazole nucleus and their cytotoxicity and toxicity evaluations. *Chemical and Pharmaceutical Bulletin*. 66(3): p. 309-318.
18. Singh A., Singh G., Bedi P.M.S., (2020) Thiophene derivatives: A potent multitargeted pharmacological scaffold. *Journal of Heterocyclic Chemistry*. 57(7): p. 2658-2703.
19. Konus M., Çetin D., Yılmaz C., Arslan S., Mutlu D., Kurt-Kızıldoğan A., Otur Ç., Ozok O., AS Algo M., Kivrak A., (2020) Synthesis, Biological Evaluation and Molecular Docking of Novel Thiophene-Based Indole Derivatives as Potential Antibacterial, GST Inhibitor and Apoptotic Anticancer Agents. *ChemistrySelect*. 5(19): p. 5809-5814.
20. Van Meerloo J., Kaspers G.J., Cloos J., Cell sensitivity assays: the MTT assay, in *Cancer cell culture*. 2011, Springer. p. 237-245.
21. Miles R., Amyes S., (1996) Laboratory control of antimicrobial therapy. *Mackie and McCartney practical medical microbiology*. 14: p. 151-178.
22. Lamour V., Hoermann L., Jeltsch J.-M., Oudet P., Moras D., (2002) An Open Conformation of the *Thermus thermophilus* Gyrase B ATP-binding Domain. *Journal of Biological Chemistry*. 277(21): p. 18947-18953.
23. Hamdouchi C., Keyser H., Collins E., Jaramillo C., De Diego J.E., Spencer C.D., Dempsey J.A., Anderson B.D., Leggett T., Stamm N.B., (2004) The discovery of a new structural class of cyclin-dependent kinase inhibitors, aminoimidazo [1, 2-a] pyridines. *Molecular cancer therapeutics*. 3(1): p. 1-9.
24. Kaminski G., Jorgensen W.L., (1996) Performance of the AMBER94, MMFF94, and OPLS-AA force fields for modeling organic liquids. *The Journal of Physical Chemistry*. 100(46): p. 18010-18013.
25. Tiwari M., Kumar A., Umre H.S., Prakash R., (2015) Microwave-assisted chemical synthesis of conducting polyindole: Study of electrical property using Schottky junction. *Journal of Applied Polymer Science*. 132(27).
26. Sundberg R., *The Chemistry of Indoles*, Academic Press, New York and London, 1970, p.

- 1; b) WA Remers. *The Chemistry of Heterocyclic Compounds, Indoles Part. 1*: p. 63.
27. Gopi D., Saraswathy R., Kavitha L., Kim D.K., (2014) Electrochemical synthesis of poly (indole-co-thiophene) on low-nickel stainless steel and its anticorrosive performance in 0.5 mol L⁻¹ H₂SO₄. *Polymer international*. 63(2): p. 280-289.
28. McCord E.F., Bucks R.R., Boxer S.G., (1981) Laser chemically induced dynamic nuclear polarization study of the reaction between photoexcited flavins and tryptophan derivatives at 360 MHz. *Biochemistry*. 20(10): p. 2880-2888.
29. Kathiravan M.K., Khilare M.M., Nikoومانesh K., Chothe A.S., Jain K.S., (2013) Topoisomerase as target for antibacterial and anticancer drug discovery. *Journal of enzyme inhibition and medicinal chemistry*. 28(3): p. 419-435.
30. Pommier Y., (2013) Drugging topoisomerases: lessons and challenges. *ACS chemical biology*. 8(1): p. 82-95.
31. Ehmann D.E., Lahiri S.D., (2014) Novel compounds targeting bacterial DNA topoisomerase/DNA gyrase. *Current opinion in pharmacology*. 18: p. 76-83.
32. Maxwell A., Lawson D.M., (2003) The ATP-binding site of type II topoisomerases as a target for antibacterial drugs. *Current topics in medicinal chemistry*. 3(3): p. 283-303.
33. Morris M.C., (2013) Fluorescent biosensors—probing protein kinase function in cancer and drug discovery. *Biochimica et Biophysica Acta (BBA)-Proteins and Proteomics*. 1834(7): p. 1387-1395.
34. Chohan T.A., Qian H., Pan Y., Chen J.-Z., (2015) Cyclin-dependent kinase-2 as a target for cancer therapy: progress in the development of CDK2 inhibitors as anti-cancer agents. *Current medicinal chemistry*. 22(2): p. 237-263.
35. Sharma S., Zhang T., Michowski W., Rebecca V.W., Xiao M., Ferretti R., Suski J.M., Bronson R.T., Paulo J.A., Frederick D., Fassl A., Boland G.M., Geng Y., Lees J.A., Medema R.H., Herlyn M., Gygi S.P., Sicinski P., (2020) Targeting the cyclin-dependent kinase 5 in metastatic melanoma. *Proceedings of the National Academy of Sciences*. 117(14): p. 8001-8012.
36. Peyressatre M., Prével C., Pellerano M., Morris M.C., (2015) Targeting cyclin-dependent kinases in human cancers: from small molecules to peptide inhibitors. *Cancers*. 7(1): p. 179-237.
37. Zhou A., Yan L., Lai F., Chen X., Goto M., Lee K.-H., Xiao Z., (2017) Design, synthesis and biological evaluation of novel indolin-2-ones as potent anticancer compounds. *Bioorganic & medicinal chemistry letters*. 27(15): p. 3326-3331.
38. Cheng D., Liu J., Han D., Zhang G., Gao W., Hsieh M.H., Ng N., Kasibhatla S., Tompkins C., Li J., Steffy A., Sun F., Li C., Seidel H.M., Harris J.L., Pan S., (2016) Discovery of Pyridinyl Acetamide Derivatives as Potent, Selective, and Orally Bioavailable Porcupine Inhibitors. *ACS medicinal chemistry letters*. 7(7): p. 676-680.
39. Lad N.P., Manohar Y., Mascarenhas M., Pandit Y.B., Kulkarni M.R., Sharma R., Salkar K., Suthar A., Pandit S.S., (2017) Methylsulfonyl benzothiazoles (MSBT) derivatives: Search for new potential antimicrobial and anticancer agents. *Bioorganic & medicinal chemistry letters*. 27(5): p. 1319-1324.
40. Morsy M.A., Ali E.M., Kandeel M., Venugopala K.N., Nair A.B., Greish K., El-Daly M., (2020) Screening and Molecular Docking of Novel Benzothiazole Derivatives as Potential Antimicrobial Agents. *Antibiotics (Basel, Switzerland)*. 9(5): p. 221.